Bridging the Pressure Gap in Water and Hydroxyl Chemistry on Metal Surfaces: the Cu(110) case

Klas Andersson,[†,‡,⊥] *Guido Ketteler,*[‖] *Hendrik Bluhm,*[§] *Susumu Yamamoto,*[†] *Hirohito Ogasawara,*[†] *Lars G. M. Pettersson,*[‡] *Miquel Salmeron,*[‖] *Anders Nilsson*[†,‡]*

[†] Stanford Synchrotron Radiation Laboratory, P.O.B. 20450, Stanford, CA 94309, USA.

[‡] FYSIKUM, Stockholm University, AlbaNova University Center, SE-10691 Stockholm, Sweden.

[‖]Lawrence Berkeley National Laboratory, Materials Sciences Division, Berkeley, CA 94720, USA.

[§] Lawrence Berkeley National Laboratory, Chemical Sciences Division, Berkeley, CA 94720, USA.

.

nilsson@slac.stanford.edu

RECEIVED DATE

Bridging the Pressure Gap: H_2O/Cu(110)

[⊥] Present address: Center for Individual Nanoparticle Functionality (CINF), Department of Physics, Technical University of Denmark, Fysikvej 312, DK-2800 Kgs. Lyngby, Denmark

*Corresponding author: Tel: +1 (650) 926 2233. Fax: +1 (650) 926 4100. E-mail: nilsson@slac.stanford.edu

Abstract

We report the first measurements on the quantitative partitioning of water between its molecular and dissociated forms at a gas-metal interface under elevated water pressures and temperatures. By means of synchrotron-based *in-situ* photoelectron spectroscopy, mixed H_2O and OH phases on Cu(110) at H_2O pressures up to 1 Torr in the 275 – 520 K temperature range are studied. In increasing order of stability three phases with H_2O:OH ratios of 2:1, 1:1 and 0:1 were observed. It was found that surprisingly large quantities of molecular water are present on the surface up to 428 K in 1 Torr H_2O. A detailed comparison with previous ultra-high vacuum (UHV) studies shows that the observed species, phases and chemical kinetics under UHV compare very well with our results at elevated pressures and temperatures. The stability of the hydrogen-bonded H_2O-OH complex at the surface, and its influence on the adsorption-desorption and dissociation kinetics, constitutes the essential link between our results and those obtained under UHV conditions.

1. Introduction

Probing the coverage, chemical speciation and phases of molecules at surfaces under realistic thermodynamic conditions is of fundamental interest in the fields of molecular environmental science, corrosion, heterogeneous catalysis and fuel cell technology. Water on metal surfaces is one of the most studied adsorption cases since the establishment of modern surface science some 25 years ago,[1,2] and a great deal has been learnt from such traditional surface science work performed under ultra-high vacuum (UHV) conditions. However, the question is how such UHV studies extrapolate towards ambient and technologically relevant conditions. This is a fundamental question that concerns the ability of the surface science approach to predict gas-surface reactions at elevated pressures. To date, no quantitative coverage determinations exist for water and the intermediates OH and O at *any* gas-metal interface under equilibrium conditions at near-ambient water partial pressures. Here we report the first such results on the water and hydroxyl chemistry on Cu(110) which is of relevance from a technological

viewpoint in both the water-gas shift (WGS) reaction[3] and methanol synthesis.[4] A detailed comparison with previous UHV work is performed.

Under UHV conditions and low temperatures (≤ 150 K) water is found to adsorb molecularly intact on clean Cu(110),[5] forming long chains along [001]; these chains are believed to consist of a zigzag arrangement of water hexamers.[6] At higher coverage these chains aggregate into a 2D structure which shows a periodicity along $[1\bar{1}0]$. The 2D periodic structure has a 7 × 8 repeat unit cell at monolayer coverage where half of the water molecules are adsorbed in an oxygen-down configuration and the other half are in a mixed H-down and H-up configuration (~2:1 ratio).[7] This intact monolayer desorbs at around 170 K in kinetic competition with dissociation,[5] forming mixed H_2O:OH phases. The activation energy for desorption is ~0.52 eV,[5] which is in good agreement with the calculated energy of adsorption.[7,8] The experimentally determined activation barrier for dissociation is close to 0.55 eV[5] which compares very well with recent theoretical results finding a dissociation barrier of 0.57 eV.[8] Note that the activation barriers reported in Ref 5 are for water in the 2-dimensional H_2O-H_2O H-bonding intact monolayer. For a water monomer the adsorption energy is significantly lower (by 0.18 eV)[8] while the barrier for dissociation is significantly larger (by 0.3 to 0.4 eV).[5,8,9] Thus, already under UHV conditions the impact on kinetic barriers by lateral H-bonding interactions is apparent.

The mixed H_2O:OH phases on Cu(110) under UHV conditions can be generated thermally, by X-ray and electron-induced damage, by co-adsorption of H_2O with small amounts of atomic O or by reacting adsorbed atomic O with atomic H, see e.g. Refs[5-7,10-17]. These mixed phases show a varying and complex thermal desorption spectroscopy (TDS) profile depending on sample preparation and heating rate.[10,14,15] The main features in TDS from the mixed phases are H_2O (m/e = 18) desorption peaks at about 200, 235 and 290 K; all at significantly higher desorption temperatures than for the molecularly intact H_2O monolayer desorbing near 170 K.[5,7,10,14,15] The 200 K and 235 K peaks are due to H_2O desorption from mixed H_2O:OH phases with characteristic low energy electron diffraction (LEED)

patterns of c(2×2)[7,10,11] and p(2×1)[10,11,16] symmetry, respectively. Above 235 K only a pure OH phase with a p(2×1) LEED pattern exists.[10-14,16] This phase decomposes near 290 K via an OH recombination mechanism in which water desorbs (OH_{ads} + OH_{ads} → H_2O_{gas} + O_{ads}),[10] leaving behind an atomic O coverage half that of the initial OH coverage in the pure OH phase.

To obtain quantitative insights into the water chemistry at elevated pressures and temperatures on metal surfaces, we have studied the water and hydroxyl chemistry on Cu(110) at near ambient conditions using X-ray photoelectron spectroscopy (XPS). XPS simultaneously allows for quantitative analysis and differentiation of chemical species. Early studies of the O_2/Ag-system proved the feasibility of recording XPS at pressures of about 1 Torr exploiting the large surface-induced core level binding energy shift to isolate contributions from surface-adsorbed species.[18,19] With advances in instrumentation coupled with the use of third-generation synchrotron radiation facilities the applicability of ambient pressure XPS has been expanded significantly.[20,21] We find a remarkably high coverage of water in mixed H_2O:OH phases on Cu(110) under near ambient partial pressures, which highlights the great importance of the strong hydrogen bond between H_2O and OH and lateral adsorbate-adsorbate H-bonding interactions at surfaces in general.

2. Experimental Section

Experiments were performed in the ambient pressure photoemission spectroscopy (APPES) endstation at the undulator beamline 11.0.2 at the Advanced Light Source (Berkeley, USA). The APPES endstation consists of two inter-connected UHV chambers, one for standard surface preparation/characterization and the other dedicated to XPS at near ambient pressures.[21] The two separate vacuum chambers have a base pressure of about 2×10^{-10} Torr. The electron spectrometer is a Specs Phoibos 150 with a custom-designed differentially-pumped electron lens. O 1s XPS spectra were recorded with a total energy resolution on the order of 350 meV.

The Cu(110) crystal was cleaned by cycles of Ar^+-sputtering and annealing to 850 K until a sharp 1×1 LEED pattern was observed. The temperature of the sample was monitored by a K-type (chromel-alumel) thermocouple located inside a special pocket of the sample for good thermal contact. The Milli-Q water (H_2O, T = 295 K) used was cleaned by multiple freeze-pump-thaw cycles and finally by distillation right before introduction into the experimental chamber.

The surface cleanliness before water adsorption was ≤ 0.03 monolayer O (1 monolayer [ML] = 1.09×10^{15} atoms cm^{-2} for Cu(110)) and no C was observed (< 0.001 ML). The small amounts of initial atomic O on the surface in most experiments may be explained by a small percentage of highly reactive defects and the unavoidable high partial pressures of water (~1×10^{-7} Torr base pressure in the XPS chamber after exposure to and evacuation from 1 Torr H_2O) to which the sample was exposed for about 600 to 1000 s during sample transfer and initial sample cleanliness characterization in the XPS chamber. We believe that these small amounts of atomic O are not affecting the results obtained at pressures seven orders of magnitude higher that produce large amounts of dissociated H_2O.

In the presence of H_2O and OH the Cu(110) surface is reactive towards residual CO. This comes as no surprise as the WGS reaction, $H_2O + CO \rightarrow H_2 + CO_2$, proceeds with a low apparent activation energy on Cu(110).[9] The levels of contribution to the O 1s XPS spectra reported here under near-ambient pressures from C-containing contaminant species (specifically -CH_3O, -HCOO and -CO_3^{2-}) were determined to be ≤ 0.03 ML. To maintain this low level of contamination the sample was frequently cleaned. In particular, for the experiments at 1 Torr, each data point corresponds to a separate experiment starting from clean Cu(110). In all cases rapid data acquisition was essential. Starting from vacuum (~10^{-7} Torr) a 1 Torr H_2O environment was reached within ~30 s and acquisition of the O 1s XPS spectrum, with an acquisition time of 60 s, then immediately started. After completion of the O 1s XPS spectrum a C 1s spectrum was recorded at once.

Quantification of the photoemission data is challenging because both gas-phase attenuation and transmission of electrons through the electron optics are energy-dependent. We overcome this problem by measuring the relative O 1s and Cu 3p signals for identical electron kinetic energies, obtained by choosing appropriate X-ray excitation energies, and calibrating against the measured O 1s to Cu 3p ratio for the saturated p(2×1)-O phase on Cu(110) generated under UHV conditions with a known coverage of 0.5 ML.[22,23] Carbon contamination levels were determined by simply relating the C 1s to O 1s XPS intensity ratio at identical kinetic energies. The C 1s to O 1s XPS intensity ratio was established by measuring surface, as well as pure gas phase, C_xO_y-species with known x:y ratio using identical experimental settings as the other experiments reported here. Coverages given in this work are estimated to be accurate within 10 %.

As discussed in Ref 5 X-ray/electron-induced dissociation of H_2O always has to be considered when using X-rays or electrons as probes. The estimated photon-flux at 735 eV, used for the O 1s XPS studies, is $4 \times 10^{14} - 3 \times 10^{15}$ photons s^{-1} cm^{-2} and the total electron yield (TEY) per photon at this photon energy is 0.035 using previously reported TEY for Cu(111).[24] We estimate the X-ray-induced electron dose during acquisition of an O 1s XPS spectrum to be 0.13 – 1.0 mC cm^{-2}, which is a significant amount.[5] To exclude beam-damage effects, we investigated water dissociation in the absence of the X-ray beam by introducing water up to pressures of 1 Torr followed by evacuation of H_2O from the chamber down to $\sim 1 \times 10^{-7}$ Torr and then recording the spectra. Similar to XPS measurements at near ambient pressures, large amounts of dissociation products (OH or O depending on sample temperature below or above 290 K) were observed. The formation rate of dissociation products at 1×10^{-7} Torr was negligible compared to high pressure exposures and we may thus conclude that water dissociation on Cu(110) occurred at similar rates whether or not X-rays were present during water dosing. Further evidence that X-ray/electron induced dissociation of water, and possible O_2-contamination in the water vapor, did not influence our results comes from comparative studies with Cu(111) where no dissociation products could be observed on the surface in XPS measurements at 1

Torr H_2O.[25] We are thus confident to claim that the results presented here are not affected by X-ray/electron-induced dissociation.

3. Results and discussion

3.1. Chemical species and phases from assignments of observed XPS peaks

In order to establish a correlation between our results and those obtained in earlier UHV studies we start by comparing XPS spectroscopic characteristics. This leads to the assignment of our observed XPS peaks under near ambient conditions to specific surface species and to their phases.

In Fig. 1 oxygen 1s XPS spectra taken in 1 Torr pressure of H_2O at temperatures in the 275 -518 K range are shown. Several O 1s XPS peaks are observed. In the spectra 1a – f, corresponding to the temperature range 275 – 430 K, we observe one peak in the range 532.65 – 533.0 eV and another at 530.8- 531.0 eV. These peaks are assigned to H_2O and OH, respectively, in good agreement with previously observed O 1s XPS binding energies for H_2O and OH coexisting at the surface in mixed H_2O:OH phases on Cu(110) under UHV and low temperature conditions.[5,12,16,17] We use the notation OH_{wmix} for the OH species at 530.8 – 531.0 eV that is H-bonding with H_2O in the mixed H_2O:OH phases.

As the H_2O coverage decreases in the temperature range 348 – 428 K (see Fig 1d – f and Fig 2), its O 1s XPS peak shifts to higher binding energy by ~0.4 eV upon transition from a 2:1 to a 1:1 H_2O:OH phase as seen in Fig 2. The same phases and binding energy shift upon transition between these phases are also observed for the data obtained at a pressure of 1×10^{-2} Torr shown in Fig. 3. We thus conclude that there are two distinctly different H_2O:OH surface phases, one with a 2:1 H_2O:OH ratio (H_2O BE ≈ 532.55 eV) saturating the surface at 1 ML and another, lower coverage phase, with a 1:1 H_2O:OH ratio (H_2O BE ≈ 532.95 eV). In Fig. 1 all spectra correspond to H_2O:OH ratios close to either 1:1 or 2:1. However, the intermediate spectrum in Fig. 3 with H_2O XPS peak binding energy about half way

between the two lower coverage 1:1 H_2O:OH spectra and the higher coverage saturated 2:1 H_2O:OH spectrum, corresponds to a near 50:50 mix of the two phases with OH_{wmix} saturated at 0.33 ML and thus displays an apparent H_2O XPS peak binding energy in between the two phases. Identical H_2O:OH phases and OH_{wmix} saturation coverage were also obtained at P = 0.2 Torr in the 300-320 K temperature range (not shown).

In the temperature range 378 – 518 K under 1 Torr pressure of H_2O (Fig. 1e – j and Fig. 2) a new spectral feature is observed at 530.45 eV which gains intensity and becomes the only distinct spectral feature observed in the range 453 – 518 K. We suggest that this peak corresponds to non-hydrogen-bonded OH in the pure p(2×1)-OH phase, in line with previous XPS assignments.[12,16,17] To further exclude the possibility that the 530.45 eV XPS peak is due to atomic oxygen, we performed experiments where the chamber was evacuated from a near ambient pressure environment at temperatures around 290 K. From UHV experiments it is well known that conversion from the p(2×1)-OH phase to atomic O is facile at temperatures around 290 K.[10,14,17] Indeed we observed dramatic differences in surface speciation after evacuation of the H_2O gas from the system depending on whether the sample temperature was below or above 290 K. The 530.45 eV species was observed after evacuation at temperatures below 290 K while atomic O, at about 529.75 eV, was observed above 290 K. At temperatures close to 285 K we could follow the conversion of the 530.45 eV species into atomic O in real time, as shown in Fig. 4. As predicted from an OH recombination mechanism ($OH_{ads} + OH_{ads} \rightarrow H_2O_{gas} + O_{ads}$), a perfect 2:1 ratio was obtained between the peak areas of the initial species with 530.45 eV binding energy, to that of the final species at 529.75 eV binding energy. These findings confirm the assignment of the species producing the 530.45 eV peak to non-hydrogen-bonded OH on Cu(110), and we therefore use the notation OH_{pure} for this OH species hereafter. We summarize the chemical species and phases from assignments of all observed XPS peaks in Table 1.[26]

On the whole, there is a close correspondence between our results and previous UHV studies regarding XPS binding energies, and hence very likely local bonding configurations, of H_2O and OH on Cu(110).

3.2. Coverages, relative stabilities and formation kinetics of observed phases

Having established the surface phases under near ambient conditions in the previous section, we will now discuss their further characteristics in terms of coverage and relative stability. Furthermore, the kinetics of OH and O formation are discussed.

For all investigated situations the maximum total surface coverage observed in the 2:1 ratio H_2O:OH phase stays close to 1 ML (± 10 %) which is also the saturation coverage observed for the molecularly intact water wetting-layer on Cu(110) under UHV conditions.[5] On the other hand, the maximum coverage observed for the 1:1 ratio H_2O:OH phase is 0.84 ML (Fig 2), i.e. this phase never forms a full monolayer under the experimental conditions explored here. Remarkably, under 1 Torr partial pressure of H_2O and a temperature as high as 428 K we still observe H_2O on our sample in the 1:1 H_2O:OH phase (see Fig 1f and Fig 2). To understand how far removed this condition is from onset of multilayer condensation of water on the surface (the dew point), we calculate the relative humidity (RH) defined as $100 \times p / p_V(T)$ where p_V is the equilibrium vapor pressure over water at a given temperature T. We come to a RH as low as 1×10^{-2} % for 1 Torr H_2O at 428 K; the dew point corresponds to 100 % RH.

We find the maximum amount of adsorbed OH to be 0.42 ML (see Fig 1d and Fig 2) but most frequently it saturated between 0.33 – 0.35 ML in the mixed H_2O:OH phases. These amounts are higher than the previously reported OH saturation coverage of 0.25 ML which was generated by H_2O + O coadsorption at low temperatures on Cu(110) under UHV conditions.[10,17] The maximum amount of OH that we observe under equilibrium conditions is in the same range as the maximum amounts of OH_{pure} that we observe after evacuation from Torr pressures at temperatures below 290 K.

With respect to atomic O, possibly very small amounts are present at the highest temperatures of 498 K and 518 K in the 1 Torr data (Fig 1i and 1j). The peak areas of atomic O in these spectra from peak-fitting analysis correspond to 0.01 ML and 0.02 ML. However, it is beyond our experimental sensitivity

to claim these amounts to be statistically significant and they are therefore not included in the decomposition in Fig. 2. However, at water partial pressures $\leq 1 \times 10^{-4}$ Torr and temperatures above 300 K (RH $< 1 \times 10^{-4}$ %) we could only observe atomic O on the Cu(110) surface.

The relative stability of the observed surface phases is apparent based on the pressure and temperature dependence in our study. The most stable phase is that of atomic O followed by OH_{pure} > 1:1 H_2O:OH > 2:1 H_2O:OH.

In Fig 1 and 2 we observe that for T > 400 K the OH (OH_{wmix} + OH_{pure}) coverage is well below its saturation coverage of about 0.33 ML. Based on the OH coverage and the time during which the sample is exposed to 1 Torr H_2O before completion of the XPS spectrum (60 s) the dissociation probability per H_2O collision with the surface (P_{diss}) can be calculated. Whether P_{diss} obtained in this way represents an absolute value or a lower limit depends on if the observed total OH coverage at a specific temperature is the result of limitations on H_2O dissociation rate or simply represents a thermodynamic equilibrium. Resolving this issue would have required time-resolved results, i.e. sequential spectra, which unfortunately at 1 Torr was not a reliable approach due to surface contamination problems in spectra beyond the first. Irrespective of the actual situation, i.e. whether the obtained P_{diss} at 1 Torr is an absolute value or possibly only a lower limit, we show that our results when compared to earlier work[5,9] are fully consistent with an auto-catalytic role of water in water dissociation. In the temperature range 470 – 520 K where water coverage is very low (<< 0.03 ML) we find P_{diss} to be $\geq 2 - 5 \times 10^{-9}$ whereas a significantly larger lower limit, $P_{diss} \geq 1.5 \times 10^{-8}$, is obtained in the temperature range 275 – 380 K where the water coverage is high (0.8-0.2 ML). From experiments with exposures to 1×10^{-2} and 0.1 Torr (Fig 3 and 4) we established P_{diss} to be as high as $1 – 5 \times 10^{-7}$ near 285 K; it could even be higher in 1 Torr at this temperature. Our results at 470-520 K ($P_{diss} \geq 2 - 5 \times 10^{-9}$) compare well with prior measurements by Nakamura et al.[9] ($P_{diss} = 5 - 50 \times 10^{-9}$). However, compared to the expected P_{diss} value of about 5×10^{-12} near 285 K arrived at by extrapolation from the 473 K $\leq$ T $\leq$ 653 K data obtained at

very low water coverage by Nakamura et al.,[9] our value obtained at high water coverage ($P_{diss} \geq 5 \times 10^{-7}$) is five orders of magnitude larger. These findings are in complete agreement with an auto-catalytic role of water in water dissociation on Cu(110) as observed in a previous UHV study.[5] Auto-catalytic water dissociation on Cu(110) is also supported by recent theoretical calculations,[8] and is discussed in more detail elsewhere.[27] Although a faster H_2O dissociation rate is expected at elevated temperatures this may be more than offset by steadily less probable H_2O-H_2O bond formation at higher temperatures due to lower H_2O coverage.

Regarding our observations for atomic O we note that although O formation via $OH_{pure} + OH_{pure} \rightarrow H_2O_{gas} + O_{ads}$ is fast above 290 K,[10,17] upon water adsorption the reverse reaction is very facile for O coverages below 0.15 ML even at 100 K.[10,17] These UHV results could explain why the equilibrium is strongly shifted towards OH under our experimental conditions. Small levels of contaminants in the chamber (mainly CO and CO_2, measured to be $\leq$ 0.1 % by gas-sampling and mass spectrometry analysis) may also affect the atomic O, and possibly OH, coverage by reacting with these water dissociation fragments at a noticeable rate above 400 K and the products leaving the surface. However, as mentioned earlier, our results on water dissociation kinetics in the 470 – 520 K range on Cu(110) in 1 Torr H_2O, discussed here and more so elsewhere,[27] are in good agreement with earlier results by Nakamura et al.,[9] indicating that the level of possible contaminants in our system has at most only a small impact on our results.

3.3. Comparison of observed water and hydroxyl surface phases to those observed under UHV conditions

Here we will compare our near ambient pressure results to the observed water and hydroxyl surface phases on Cu(110) under UHV conditions. The phases will be discussed in their relative order of stability.

3.3.1. OH_{pure} adsorption and the Cu(110) surface

The p(2×1)-LEED OH_{pure} phases on both Cu(110)[14] and Ni(110)[28] show the same characteristic 2-spot electron-stimulated desorption (ESD) pattern, derived from OH inclined along the two [001] azimuthal directions (i.e. perpendicular to close-packed atomic rows), suggesting the same type of adsorption site for OH_{pure} on the two surfaces. Based on time-of-flight spectrometry[29] the adsorption site of OH_{pure} in the p(2×1)-LEED phase has been proposed to be the short-bridge site on the non-reconstructed Ni(110) surface. The same OH_{pure} adsorption site was found to be the most favorable on Cu(110) based on density functional theory (DFT) modeling.[8] In our XPS studies the binding energy of OH_{pure} does not change when going from vacuum conditions at 285 K to 1 Torr H_2O and 520 K. This strongly suggests that the favored Cu(110)-OH_{pure} local bonding configuration is identical under both UHV conditions and at elevated pressures and temperatures.

3.3.2. The 1:1 H_2O:OH phase

The stable 1:1 H_2O:OH phase observed in our experiments compares very well with characteristics of the p(2×1)-LEED mixed H_2O:OH phase which is the most stable mixed H_2O:OH phase on Cu(110) under UHV conditions. In fact, Polak[14] found a 1:1 ratio between H_2O and OH in the p(2×1)-LEED mixed H_2O:OH phase based on analysis of TD spectra. These findings were later corroborated in an XPS study by Ammon et al.[16]

Polak suggested the structure of the 1:1 H_2O:OH phase to consist of H_2O-OH chains oriented along the close-packed Cu rows with a 1-dimensional periodicity of twice the Cu-Cu distance.[14] The 1-dimensional nature of the 1:1 H_2O:OH phase along $[1\bar{1}0]$ is consistent with observations of a p(2×1) LEED pattern showing streaks in the [001]-direction.[11,16] ESD results implied that the H_2O molecules lie flat and are H-bonded to OH to form a H_2O-OH chain.[14] Furthermore, the 2-spot ESD pattern from the 1:1 H_2O:OH phase was interpreted as due to uncoordinated H in OH inclined along the two [001] azimuthal directions at about 35° from the surface normal since it is identical to the 2-spot ESD pattern

for the p(2×1)-LEED OH phase.[14] The arrangement of H-bonds in the chain model proposed by Polak would be in agreement with OH on metal surfaces being a good H-bond acceptor, and relatively bad donor, towards H_2O.[27]

3.3.3. The 2:1 H_2O:OH phase

It is evident from TDS[10,14] and XPS[12,16] under UHV that compared to the 1:1 phase discussed above, the c(2×2) mixed H_2O:OH phase contains significantly more H_2O which also is less tightly bound at the surface. Consistent with these observations and our findings discussed in Section 3.2., the 2:1 H_2O:OH phase we observe compares favorably with the c(2×2)-LEED mixed H_2O:OH phase previously observed in UHV experiments. The geometry of this c(2×2) phase is dictated by the oxygen atoms alone because LEED is largely insensitive to H. Furthermore, both H_2O and OH are essentially lying flat on the surface because no OD-stretch from either uncoordinated D in D_2O or OD was observed in IR-studies[13] when D_2O was adsorbed onto the pure OD phase and the sample was kept below 195 K. Recent theoretical work also supports a near-planar geometry for all internal OH-groups in OH and H_2O in a fully saturated (1 ML) mixed H_2O:OH phase on Cu(110), although only the 1:1 H_2O:OH ratio phase was considered.[8]

The 2:1 H_2O:OH phase forms by saturating the incomplete H-bonding network of the 1:1 H_2O:OH phase. The coordinative differences due to the closing of the H-bonding network may explain the observed changes in XPS binding energy for H_2O. We do not exclude that there may also be changes in adsorption sites upon transition from the 1:1 H_2O:OH phase to the 2:1 H_2O:OH phase on Cu(110).

3.4. Stability of the H_2O-OH complex

So far we have not yet provided an explanation for the surprisingly high coverages of H_2O on Cu(110) under the investigated conditions. Based on the UHV studies discussed in the Introduction it is essential to account for the proper H-bonding interactions and energetics when considering kinetic barriers. Here we assess the kinetic information available from previous UHV work, focusing on the 1:1 H_2O:OH phase on Cu(110) from which water desorbs near 235 K in UHV leaving OH_{pure} on the surface. A quantitative comparison is made to our near ambient pressure results and the importance of adsorbed OH as anchoring and clustering site for H_2O is discussed.

The peak desorption temperature of H_2O under UHV from the 1:1 H_2O:OH phase at 235 K shows very small to no coverage dependence[10,14,15] (unless high initial coverages of atomic O [> 0.15 ML] are pre-adsorbed on Cu(110))[10] which validates the assumption of first-order desorption kinetics. Based on the TDS data[10] the activation barrier for desorption can be calculated[30] using the experimentally determined range for the pre-exponential factor (υ) for H_2O of $10^{15 \pm 1}$ s^{-1}.[31-33]

The 235 K H_2O TDS-peak leads to an activation barrier for desorption of 0.18 ± 0.01 eV (for $\upsilon = 10^{15\pm1}$ s^{-1}) higher than that from the molecularly intact monolayer (T_{des} = 175 K)[10] where the H-bonding interactions are only of H_2O-H_2O character. These results can be interpreted in a model where the rate-limiting step for H_2O-desorption involves escaping a potential well defined by the bonding to Cu and, in addition, a bond to OH which is about 0.2 eV stronger than the H_2O-H_2O bond. Based on these assumptions, we find the numerical results to be fully consistent with recent theoretical work on the Pt(111) surface where the H_2O-OH H-bond strength was also found to be ~0.2 eV stronger than the H_2O-H_2O H-bond.[34,35]

With the result above establishing the stability of the H_2O-OH complex we test whether this accounts for the observed coverages of H_2O in our experiments. The desorption barrier for H_2O in the 1:1 H_2O:OH UHV phase was calculated to be 0.69 ± 0.045 eV (for $\upsilon = 10^{15\pm1}$ s^{-1}) from data in Ref.[10] Using this derived desorption barrier for the low, but still surprisingly high, coverage of 0.04 ML H_2O in the 1:1 H_2O:OH phase at 428 K and P = 1 Torr (Fig. 1f and Fig. 2), we calculate a H_2O desorption rate of 1.4 - 13 × 10^5 ML s^{-1} as obtained from the first-order Polanyi-Wigner equation.[36] This result is in very good agreement with the actual impingement rate for H_2O of 4.3 × 10^5 ML s^{-1} at 1 Torr.[37] Equally good agreement is reached for the data at T = 378 K and P = 1 Torr (Fig 1e and Fig 2). These comparisons show that the UHV results extrapolated to elevated pressures and temperatures are in very good quantitative agreement with our experimental observations on adsorption-desorption equilibrium

kinetics. Furthermore, they prove that the H-bonding interaction between H_2O and OH is responsible for the observed kinetics and unexpectedly high H_2O coverages.

Assuming that the adsorption energy of water closely corresponds to the activation barrier for desorption ($E_{ads} \sim -E_a^{des}$), which is the case for the intact monolayer,[5,7,8] we can directly compare the calculated adsorption energy for a H_2O monomer on Cu(110) of 0.375 eV[8] to that of 0.69 ± 0.045 eV for H_2O complexed with OH in the 1:1 H_2O:OH phase. We realize that the strongly adsorbed OH groups function as anchoring and clustering sites for H_2O, increasing its surface residence time by many orders of magnitude and promoting high local concentrations of H_2O. This, in turn, increases the formation probability of H_2O-H_2O H-bonding complexes which lower the dissociation barrier. The importance of adsorbed OH groups for water adsorption-desorption kinetics on metal surfaces has very recently been further demonstrated by comparing near ambient results on Cu(110) with the clean Cu(111) surface where on the latter no adsorbed H_2O was observed;[25] the difference was determined to be due to kinetic limitations on the OH formation (H_2O dissociation) rate on Cu(111).

The stability of the H_2O-OH complex at the surface not only slows down the water desorption rate drastically, we strongly believe that it also is the microscopic origin of the auto-catalytic water dissociation. As the H_2O-OH H-bond is significantly stronger than the H_2O-H_2O bond it provides a significant stabilization of the dissociated state compared to in water monomer dissociation and hence constitutes the necessary thermodynamic driving force for an activation barrier lowering.[27] It is clear that via the stability of the H_2O-OH complex at the surface a very close connection can be made between our observations at elevated pressures and temperatures and those previously obtained from traditional surface science work.

4. Conclusions

The quantitative partitioning of water between its molecular and dissociated forms on a metal surface at elevated temperatures and pressures has been explored. The chemistry and coverage of H_2O- and OH-species on Cu(110) under adsorption-desorption equilibrium conditions at near ambient H_2O partial pressures in the temperature range 275 – 520 K was reported.

Besides non-H-bonded OH in the pure OH phase, we also observe a stable 1:1 H_2O:OH phase which, upon further accumulation and saturation of H_2O forms a less stable 2:1 H_2O:OH phase. The local bonding configurations (XPS characteristics), H_2O:OH ratios and relative stability of the observed phases compare very well with studies under UHV conditions. A very good quantitative agreement between our results and earlier UHV work with respect to water desorption kinetics was reached when accounting for the attractive H-bonding interaction between adsorbed H_2O and OH, deduced to be ~0.2 eV stronger than H_2O-H_2O on Cu(110). The energetic difference in H-bond strength is very likely the thermodynamic driving force responsible for the observed auto-catalytic water dissociation. Our findings provide strong support for the traditional surface science approach performed under UHV and at moderate temperatures but also shows that in order to fully account for the range of observed water chemistry in our study it is of utmost importance to take into account the proper lateral H-bonding interactions.

The results are of general importance to gas-surface reactions involving not only water on Cu(110). The stability of the H_2O-OH complex lowers the desorption kinetics for H_2O significantly. By reacting with atomic O to form OH_{pure} with which H_2O can form a stable complex, an H_2O-rich environment can lower the availability of OH_{pure} and atomic O for participation in surface reactions. The stability of the H_2O-OH complex may in this respect possibly poison catalytic processes which rely on a supply of OH_{pure} and atomic O. On the other hand, a H_2O-H_2O H-bonding complex can promote the formation of OH in an auto-catalytic way. A sensitive interplay between kinetically promoting and poisoning effects,

stemming from H-bonding interactions, is thus an integral part of water and hydroxyl chemistry at surfaces.

Acknowledgements

This work was supported by the National Science Foundation under contract NSF-CHE-0431425; the Director, Office of Energy Research, Office of Basic Energy Sciences, Chemical Sciences Division and Materials Sciences Division of the U.S. Department of Energy under contract DE-AC02-05CH11231 and under the auspices of the President's Hydrogen Fuel Initiative; the Swedish Foundation for Strategic Research and the Swedish Natural Science Research Council. GK thanks the Alexander-von-Humboldt foundation for financial support.

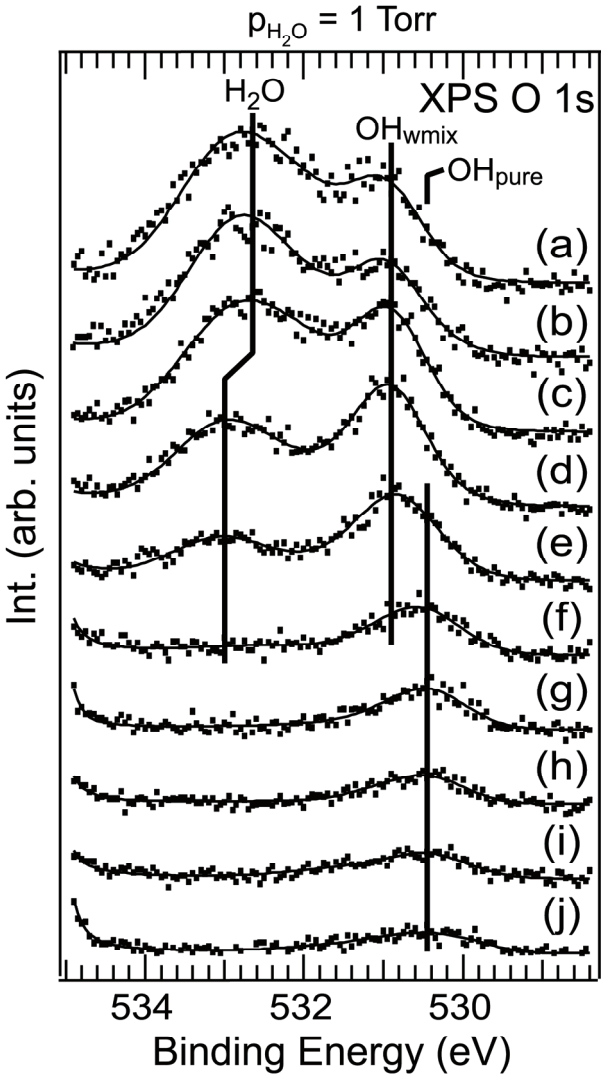

Figure 1. O 1s XPS recorded in 1 Torr partial pressure of H_2O and sample temperature in the 275 - 518 K range. (a) 275 K, (b) 301 K, (c) 323 K, (d) 348 K, (e) 378 K, (f) 428 K, (g) 453 K, (h) 483 K, (i) 498 K and (j) 518 K. The gas-phase peak of H_2O located above 535 eV is not shown. The marked spectral features for OH_{wmix} and OH_{pure} are for OH-species H-bonding with H_2O or not, respectively. The observed binding energy shift for the H_2O component is due to the transition from a 2:1 ratio H_2O:OH_{wmix} phase to a more stable 1:1 ratio H_2O:OH_{wmix} phase at higher temperatures as discussed in the text. The spectra are normalized with respect to coverage and the result from a least-square peak-fitting procedure, after Shirley background subtraction and using the components listed in Table 1, is shown as a thin solid line as a guide to the eye for each spectrum.

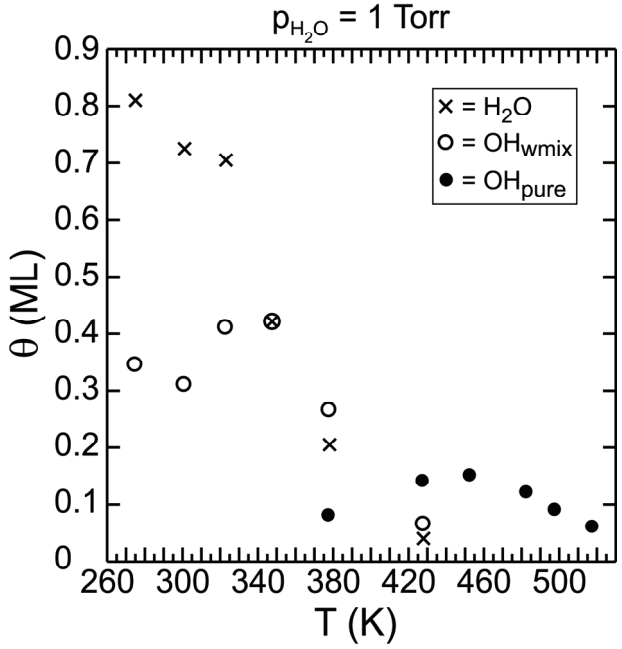

Figure 2. Partial coverages for surface species observed in the O 1s XPS spectra presented in Fig 1 recorded at 1 Torr partial pressure of H_2O and Cu(110) sample temperatures in the 275 – 518 K range. Note the identical coverage of H_2O (crosses) and OH_{wmix} (open circles) at 348 K. The nomenclature used for the OH-species, OH_{wmix} and OH_{pure} (filled circles), are for OH-species H-bonding with H_2O or not, respectively.

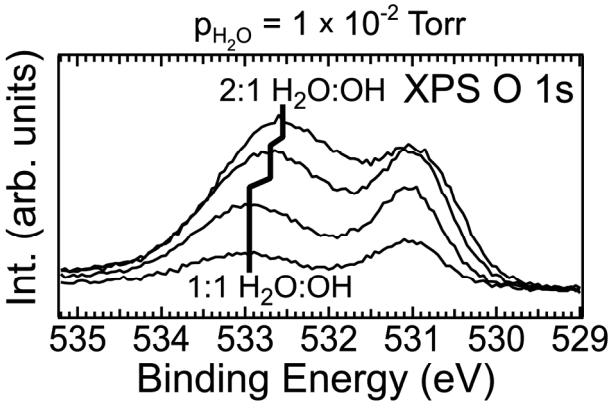

Figure 3. Selected O 1s XPS spectra showing the spectral change in H_2O (and OH_{wmix}) going from the 1:1 H_2O:OH surface phase to the 2:1 H_2O:OH surface phase on Cu(110). Spectra were recorded for decreasing temperatures 295 down to 273 K in a 1×10^{-2} Torr partial pressure of H_2O.

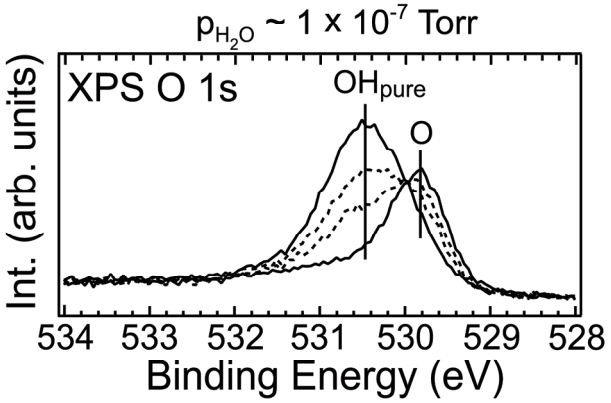

Figure 4. Selected O 1s XPS spectra showing the 2:1 conversion from OH_{pure} (0.2 ML) to atomic O slowly occurring at 285 K. A ~5 s exposure of the Cu(110) sample to a 0.1 Torr partial pressure of H_2O was immediately followed by evacuation down to approximately 1×10^{-7} Torr after which the XPS spectra were recorded.

Table 1. O 1s XPS spectral characteristics for all components observed under the varying conditions at the Cu(110) surface.[a]

Species / Phase	Gaussian FWHM (eV)	Binding Energy (eV)
H_2O (H_2O:OH = 2:1)	1.7 ± 0.1	532.55 ± 0.1
H_2O (H_2O:OH = 1:1)	1.7 ± 0.1	532.9 ± 0.1
OH_{wmix}	0.95 ± 0.15	530.95 ± 0.1
OH_{pure}	0.95 ± 0.05	530.45 ± 0.05
O	0.65 ± 0.05	529.75 ± 0.05

[a] A Lorentzian FWHM of 0.15 eV was used for all components to account for the O 1s core hole life-time. A generic asymmetric line-shape, determined for each component in situations where they were very well-resolved, was used to account for vibrational structures and electron-hole pair excitations around E_F at the Cu(110) surface.

REFERENCES

(1) Thiel, P. A.; Madey, T. E. *Surf. Sci. Rep.* **1987**, *7*, 211.

(2) Henderson, M. A. *Surf. Sci. Rep.* **2002**, *46*, 1.

(3) Schumacher, N.; Boisen, A.; Dahl, S.; Gokhale, A.A.; Kandoi, S.; Grabow, L.C.; Dumesic, J.A.; Mavrikakis, M.; Chorkendorff, I. *J. Catal.* **2005**, *229*, 265.

(4) Yoshihara, J.; Campbell, C.T.; *J. Catal*. **1996**, *161*, 776.

(5) Andersson, K.; Gómez, A.; Glover, C.; Nordlund, D.; Öström, H.; Schiros, T.; Takahashi, O.; Ogasawara, H.; Pettersson, L.G.M.; Nilsson, A. *Surf. Sci.* **2005**, *585*, L183.

(6) Yamada, T.; Tamamori, S.; Okuyama, H.; Aruga, T. *Phys. Rev. Lett.* **2006**, *96*, 036105.

(7) Schiros, T.; Haq, S.; Ogasawara, H.; Takahashi, O.; Öström, H.; Andersson, K.; Pettersson, L.G.M.; Hodgson, A.; Nilsson, A. *Chem. Phys. Lett.* **2006**, *429*, 415.

(8) Ren, J.; Meng, S. *J. Am. Chem. Soc.* **2006**, *128*, 9282.

(9) Nakamura, J.; Campbell, J.M.; Campbell, C.T. *J. Chem. Soc. Faraday Trans.* **1990**, *86*, 2725.

(10) Bange, K.; Grider, D.E.; Madey, T.E.; Sass, J.K. *Surf. Sci.* **1984**, *136*, 38.

(11) Spitzer, A.; Lüth, H. *Surf. Sci.* **1982**, *120*, 376.

(12) Spitzer, A.; Lüth, H. *Surf. Sci.* **1985**, *160*, 353.

(13) Kubota, J.; Kondo, J.; Domen, K.; Hirose, C. *Surf. Sci.* **1993**, *295*, 169.

(14) Polak, M. *Surf. Sci.* **1994**, *321*, 249.

(15) Kolovos-Vellianitis, D.; Küppers, J. *J. Phys. Chem. B* **2003**, *2559*, 107.

(16) Ammon, Ch.; Bayer, A.; Steinrück, H.P.; Held, G. *Chem. Phys. Lett.* **2003**, *377*, 163.

(17) Clendening, W.D.; Rodriguez, J.A.; Campbell, J.M.; Campbell, C.T. *Surf. Sci.* **1989**, *216*, 429.

(18) Nilsson, A. *J. El. Spec. Rel. Phenom.* **2002**, *126*, 3; Nordfors, D.; Mårtensson, N.; A. Nilsson **1986**, unpublished.

(19) Joyner, R.W.; Roberts, M.W. *Chem. Phys. Lett.* **1979**, *60*, 459

(20) Ogletree, D.F.; Bluhm, H.; Lebedev, G.; Fadley, C.S.; Hussain, Z.; Salmeron, M. *Rev. Sci. Instrum.* **2002**, *73*, 3872.

(21) Bluhm, H.; Andersson, K.; Araki, T.; Benzerara, K.; Brown, G. E.; Dynes, J. J.; Ghosal, S.; Gilles, M. K.; Hansen, H.-Ch.; Hemminger, J. C.; Hitchcock, A. P.; Ketteler, G.; Kilcoyne, A. L. D.; Kneedler, E.; Lawrence, J. R.; Leppard, G. G.; Majzlam, J.; Mun, B. S.; Myneni, S. C. B.; Nilsson, A.; Ogasawara, H.; Ogletree, D. F.; Pecher, K.; Salmeron, M.; Shuh, D. K.; Tonner, B.; Tyliszczak, T.; Warwick, T.; Yoon, T. H. *J. Electron. Spectrosc. Relat. Phenom.* **2006**, *150*, 86.

(22) Coulman, D. J.; Wintterlin, J.; Behm, R. J.; Ertl, G. *Phys. Rev. Lett.* **1990**, *64*, 1761.

(23) Jensen, F.; Besenbacher, F.; Laegsgaard, E.; Stensgaard, I. *Phys. Rev. B* **1990**, *41*, 10233.

(24) Henneken, H.; Scholze, F.; Ulm, G. *J. Electron. Spectrosc. Relat. Phenom.* **1999**, *101-103*, 1019.

(25) Yamamoto, S.; Andersson, K.; Bluhm, H.; Ketteler, G.; Starr, D.E.; Schiros, T.; Ogasawara, H.; Pettersson, L.G.M.; Salmeron, M.; Nilsson, A. *J. Phys. Chem. C* **2007**, *111*, 7848.

(26) An exception, compared to all other recorded H_2O XPS peaks, is the 0.2 eV broader FWHM of the H_2O peak in the spectrum in Fig 1a (1 Torr and 275 K, RH = 22 %) which most likely contains some small amounts of H_2O on top of the 2:1 H_2O:OH phase (see Fig 2).

(27) Andersson, K.; Ketteler, G.; Bluhm, H.; Yamamoto, S.; Ogasawara, H.; Pettersson, L.G.M.; Salmeron, M.; Nilsson, A. *submitted*.

(28) Benndorf, C.; Madey, T.E. *Surf. Sci.* **1988**, *194*, 63.

(29) Roux, C.D.; Bu, H.; Rabalais, J.W. *Surf. Sci.* **1992**, *279*, 1.

(30) Chorkendorff, I.; Niemantsverdriet, J.W. *Concepts of Modern Catalysis and Kinetics*, Wiley-VCH, 2003.

(31) Daschbach, J.L.; Peden, B.M.; Smith, R.S.; Kay, B.D. *J. Chem. Phys.* **2004**, *120*, 1516.

(32) Brinkley, D.; Dietrich, M.; Engel, T.; Farrall, P.; Gantner, G.; Schafer, A.; Szuchmacher, A. *Surf. Sci.* **1998**, *395*, 292.

(33) Delval, C.; Rossi, M.J. *Phys. Chem. Chem. Phys.* **2004**, *6*, 4665.

(34) Karlberg, G. S.; Wahnström, G. *Phys. Rev. Lett.* **2004**, *92*, 136103.

(35) Karlberg, G.S.; Wahnström, G. *J. Chem. Phys.* **2005**, *122*, 194705.

(36) King, D.A. *Surf. Sci.* **1975**, *47*, 384.

(37) The actual *adsorption* rate is determined by the sticking (trapping) coefficient S and appears to be near unity (i.e. $S \approx 1$) for H_2O impinging the structurally (and charge-) corrugated hydroxylated Cu(110) surface considering the adsorption rate seemingly not limiting the overall surface chemical kinetics. In fact, a trapping coefficient as high as unity (i.e. $S = 1$), for all coverages of H_2O investigated, was measured for temperatures up to 600 K on the corrugated, and most likely hydroxylated, TiO_2(110) surface.[32]